



Equilibrium modeling and thermodynamic parameters for adsorption of cationic dyes onto Yemen natural clay

Mamdouh Mahmoud Nassar^{a,*}, Mohammad Shawky El-Geundi^a,
Abdulrakib Abdelwahab Al-Wahbi^b

^aFaculty of Engineering, Chemical Engineering Department, El-Minia University, El-Minia, Egypt
Tel. +20 2 86 23423337; Fax: 020862346674; email: mamdouh_nassar@yahoo.com

^bFaculty of Petroleum and Engineering, Chemical Engineering Department, Hadramout University of Science and Technology, Al-Mukalla, Hadramout, Republic of Yemen

Received 29 April 2011; Accepted 30 January 2012

ABSTRACT

The equilibrium modeling for adsorption of cationic dye Methylene Blue (MB) onto Yemen natural clay at different temperatures, particle size and solution pH was studied. The adsorption capacity was found to be increase with increasing temperature and pH and decreased with increasing particle size. The maximum adsorption capacity was 500.0 (mg g⁻¹) at $T = 25^{\circ}\text{C}$, $d_p = 250\text{--}355\ \mu\text{m}$ and $\text{pH} = 12$. The data are successfully tested by Langmuir, Freundlich, Temkin and Redlich–Peterson models. It was found that the Redlich–Peterson isotherm best fit the experimental data over the whole concentration range. Thermodynamic parameters such as standard Gibbs free energy (ΔG°), standard enthalpy (ΔH°), and standard entropy (ΔS°) were calculated. The thermodynamic parameters of methylene blue/clay system indicated spontaneous and endothermic nature of the adsorption process. The results demonstrate that Yemen natural clay is very effective in the removal of MB from aqueous solution and can be used as alternative of high cost commercial adsorbents.

Keywords: Equilibrium adsorption; pH; Modeling; Thermodynamic parameters; Methylene Blue; Yemen natural clay

1. Introduction

Colored wastewater from various industries like textiles, pulp mills, leather, printing, food, and plastics have been a serious environmental problem. It is estimated that 1–1.5% of the dye is lost during dyeing and finishing process and is released into wastewater. The presence of very small amounts of dyes in water (less than 1 ppm for some dyes) is highly visible and undesirable [1,2]. The textile industry utilizes about 100,000

commercially available synthesis dyes and more than 7×10^5 t/y are produced annually [3].

Dye bath effluents impart color to receiving streams and affect its esthetic value. Color interferes with penetration of sunlight into water, retards photosynthesis, inhibits the growth biota and interferes with oxygen solubility in water bodies [4]. Conventionally chemical, biological and physical methods have been employed for dye removal, such as coagulation, flocculation, advanced oxidation, electrocoagulation and adsorption [5–7]. Adsorption offers advantages in terms of low initial cost, flexibility, simplicity of design, ease of operation and insensitivity to

*Corresponding author.

toxic pollutants and does not result in the formation of harmful substances [5].

Most of work on adsorption has been undertaken using activated carbon which is costly and required regeneration. Hence the research is being conducting for low-cost adsorbents, including raw agricultural solid wastes such as maize cob [8], palm-fruit bunch particles [9], bagasse pith [10], sawdust [11], papaya seeds [12], hazelnut shell [13].

Clay has been increasingly paid attention because of its low cost, abundance, high specific surface area and mechanical stabilities. In addition, clay has shown good results as an adsorbent for the removal of various metals [14], surfactants [15], and basic and acid dyes [16].

The study was aimed to quantitatively compare the applicability of different models (Langmier, Freundlich, Temken, and Ridlich–Petreson isotherms) using the average relative error analyses. Furthermore, equilibrium modeling and thermodynamic parameters were deeply discussed to understand the mechanism of adsorption of MB onto Yemen clay.

2. Material and methods

2.1. Materials

The natural clay used was collected from Al-Rayan zone, Al-Mukalla City, Hadramout Governorate, Republic of Yemen. The adsorbent was washed, crushed and sieved through different standard sieves into the desired particle size and used without any pre-treatment. The resulting sample was dried at 105°C and stored in sealed containers prior to use.

Methylene Blue [C.I. Basic Blue 9, C₁₆H₁₈N₃SCl, M.W. = 319.9 g mol⁻¹, and λ_{max}: 665 nm] supplied by Merck company (Germany) was used as adsorbate. The chemical structure of MB is shown in Fig. 1.

2.2. Characterization of natural clay

Chemical composition of natural clay was determined using XR-F Spectrometer, ARL 9800, Switzerland.

Solid density, particle density and porosity for natural clay were determined using mercury Poresizer 9320, Micromertics, USA.

The surface physical properties such as specific surface area, pore size distribution (PSD) and total pore

volume were measured by nitrogen adsorption–desorption isotherms using a multipurpose apparatus Nova 2000 analyzer, Quantachrome Instruments, Japan. A BET analysis based on the amount of N₂ gas adsorbed at various partial pressures was used to determine the surface area (S_{BET}). The single condensation point (p/p₀ = 0.95) was used to find the total pore volume (V_T). The average pore radius (r_{av}) was calculated using total surface area and total pore volume (r_{av} = 2V_T/S_{BET}). The volumes of micropores, mesopores, and macropores were calculated from N₂ adsorption isotherm by applying the Barrett–Joyner–Hallenda (BJH) method [17].

Mineralogical analysis (XRD analysis) was determined using Panalytical X'Pert PRO X-ray diffractometer.

2.3. Method

Batch adsorption experiments were carried out and the adsorption capacity of clay was determined by contacting a constant mass (0.05 g) of clay with a fixed volume (50 ml) of MB solution in sealed glass bottles of different initial concentrations of dye solution (50–700 mg dm⁻³). The bottles were agitated in an isothermal water-bath shaker for 5 h until equilibrium was reached. At the end of the adsorption time, a known volume of the solution was removed and centrifuged (5000 rpm for 10 min) for analysis of the supernatant.

The concentration of MB in aqueous solution was determined at λ_{max} = 665 nm using double beam UV–visible spectrophotometer (Shimadzu, Model UV 1601, Japan).

The amount of MB adsorbed onto clay, q_e (mg g⁻¹), was calculated by the following equation:

$$q_e = \frac{(C_0 - C_e) \times V}{m} \quad (1)$$

where C₀ and C_e are the initial and equilibrium concentrations of dye solution (mg dm⁻³), respectively. V is the total volume of the dye solution (dm³), and m is the mass of clay used (g).

3. Results and discussion

3.1. Characterization of natural clay

Chemical analysis indicates the following composition: SiO₂, 62.38%; Al₂O₃, 13.60%; Fe₂O₃, 7.05%; CaO, 3.75%; MgO, 3.11%; K₂O, 2.63%.

The N₂ adsorption–desorption isotherm obtained for the clay is shown in Fig. 2. As shown in the Figure, the desorption branch of this isotherm exhibited hysteresis and correspond to the Type IV isotherm. The existence of the hysteresis loop in the isotherm is due to the capillary condensation of N₂ gas occurring in the mesopores and therefore, the Type IV isotherm is considered

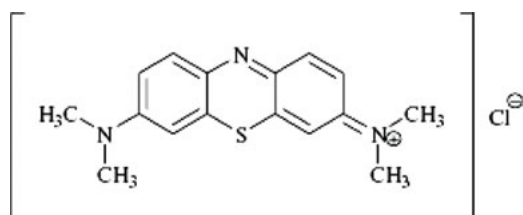


Fig. 1. The chemical structure of methylene blue.

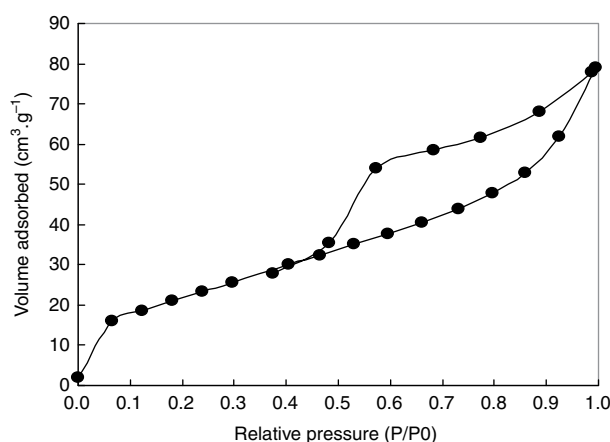


Fig. 2. Adsorption isotherms of clay tested with N_2 at 77.35 K.

as the characteristic feature of the mesoporous materials [18]. The sharp rise near $P/P_0 = 0.4$ corresponds to condensation in the primary mesopores. Physical characteristics of the natural clay such as the values of BET surface area (S_{BET}), total pore volume (V_T), micropore volume (V_{mic}), mesopore volume (V_{mes}), macropore volume (V_{mac}), and average pore radius (r_{av}) are listed in Table 1. Data in Table 1 indicate that natural clay has high specific surface area ($82.3 \text{ m}^2 \text{ g}^{-1}$) and total pore volume ($0.109 \text{ cm}^3 \text{ g}^{-1}$).

Fig. 3 shows PSD of clay calculated from N_2 adsorption isotherm by applying the Barrett–Joyner–Hallenda (BJH) method [17]. As illustrated in Fig. 3, pores between 1.4 and 2.9 nm were dominant. Their average pore size is 2.15 nm, which was in the mesopore range (pore size, 2–50 nm).

Mineralogical analysis (XR-D analysis) proved that clay is composed of montmorillonite and illite as clay minerals and quartz and gypsum as non-clay minerals.

3.2. Adsorption isotherms

Determining the distribution of MB between natural clay and the liquid phase when the system is at state of

Table 1

Surface characteristics of natural clay

Total surface area (S_{BET}) ($\text{m}^2 \text{ g}^{-1}$)	82.34
Total pore volume (V_T) ($\text{cm}^3 \text{ g}^{-1}$)	0.109
Average pore radius (r_{av}) (\AA)	26.40
Micropore volume (V_{mic}) ($\text{cm}^3 \text{ g}^{-1}$)	0.012
Mesopore volume (V_{mes}) ($\text{cm}^3 \text{ g}^{-1}$)	0.096
Macropore volume (V_{mac}) ($\text{cm}^3 \text{ g}^{-1}$)	0.001
Solid-phase density (ρ_s) (g cm^{-3})	2.526
Particle density (ρ_p) (g cm^{-3})	1.859
Particle porosity (ϵ_p)	0.264

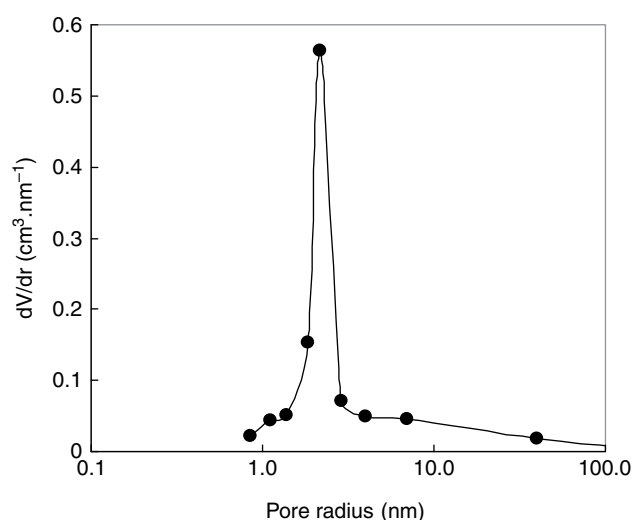


Fig. 3. Pore size distributions of clay determined by using BJH technique.

equilibrium is important in establishing the capacity of the clay for MB. Preliminary experiments showed that such equilibrium was established within 180 min; however, all equilibrium experiments were allowed to run for 300 min.

Plotting the amount of MB adsorbed at equilibrium (q_e) against final concentration in the aqueous phase (C_e) at different temperatures, different particle size and different pH gave a characteristic H-shaped curve as shown in Figs. 4–6. According to the slope of the initial portion of the curve of MB onto clay, this isotherm may be classified as H-shape according to Giles classification [19]. In this type of isotherm, the initial portion provides information about the availability of the active sites to the adsorbate and the plateau signifies the monolayer formation. The initial curvature indicates that a large amount of dye is adsorbed at a lower concentration as more active sites of clay are available. As the concentration increases, it becomes difficult for dye molecule to find vacant sites, and so monolayer formation occurs [19].

3.2.1. Effect of temperature

Fig. 4 present the adsorption isotherms of MB onto clay at different temperatures (15°C , 25°C , 35°C and 45°C) at constant particle size 250–350 μm and $\text{pH} = 6 \pm 0.2$. From this Figure, it can be seen that adsorption capacity of clay increased from 420.0 to 471.4 mg g^{-1} with an increase in temperature of solution from 15°C to 45°C .

The enhancement in the adsorption capacity may be due to increasing the rate of diffusion of the adsorbate molecules across the external boundary layer and in the internal pores of the adsorbent particle, owing to the decrease in the viscosity of the solution [20]. Senthilkumar et al. [21]

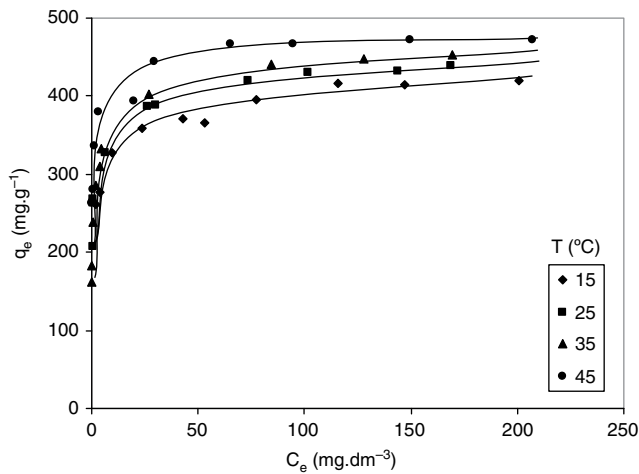


Fig. 4. Adsorption Isotherms of MB onto Clay at different temperatures. Particle diameter = 250–355 μm , pH = 6 + 0.2, mass of clay = 0.05 g and solution volume = 0.05 dm^3 .

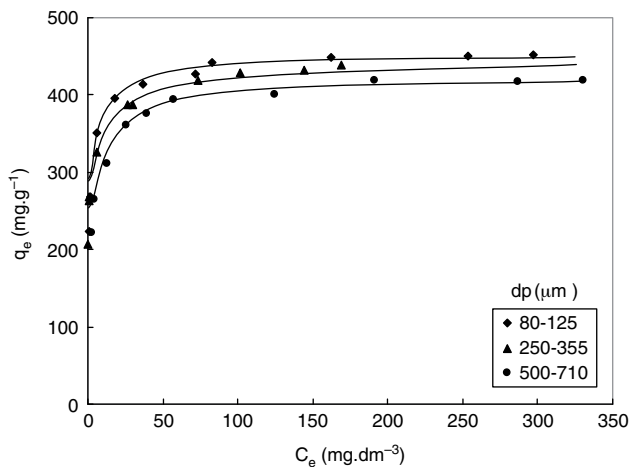


Fig. 5. Adsorption isotherms of MB onto clay at different particle size. pH = 6 + 0.2, mass of clay = 0.05 g and temperature = 25°C \pm 1°C and solution volume = 0.05 dm^3 .

suggested that the increase in adsorption capacity with increase in temperature might be due to the increase in the total pore volume of the adsorbent, an increase of number of active sites for the adsorption as well as an increase in the mobility of the MB molecules.

Increase of the adsorption capacity of clay by raising temperature indicates a chemisorptions mechanism, with an increasing number of molecules acquiring sufficient energy to undergo chemical reaction with clay. This conclusion was confirmed by the change in standard enthalpy (ΔH°) during the adsorption processes. Standard enthalpy change (ΔH°) at different temperatures has been calculated using Van't Hoff equation and was found to be 32.3 kJ g mol^{-1} . Similar results show that the adsorption process of MB is an endothermic in nature [22].

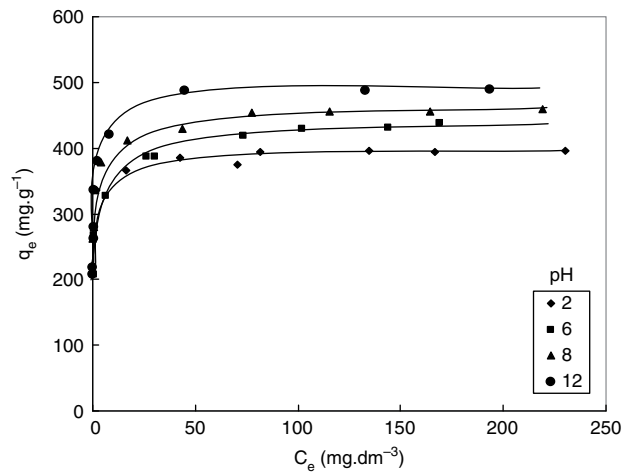


Fig. 6. Adsorption isotherms of MB onto clay at different solution pH values. Particle diameter = 250–355 μm , mass of clay = 0.05 g and temperature = 25°C \pm 1°C and solution volume = 0.05 dm^3 .

3.2.2. Effect of particle size

Fig. 5 shows that a decrease in clay particle size led to an increase in equilibrium adsorption capacity. The experimental equilibrium adsorption capacity of clay for MB increased from 419.4 to 452.2 mg g^{-1} with decreasing particle size from 500–710 to 80–125 μm . Similar results have been obtained by several investigators [23,24]. This behavior can be attributed to breaking up large particle diameter to form smaller ones probably serves to open some tiny, sealed pores in the clay which become available for adsorption, thus slightly increasing the total specific surface area of a given mass [25].

3.2.3. Effect of pH

Fig. 6 shows the effect of pH on adsorption capacity of clay for MB over a wide pH range of 2–12. As shown in the Figure, a strong dependence of equilibrium capacity on the solution pH. The adsorption capacity increased from 395.9 to 489.5 mg g^{-1} with increasing solution pH from 2 to 12. The dependence of adsorption on pH could be attributed to the fact that the surface charge of clay was greatly affected by solution pH. According to Özdemiş et al. [26] when the solution pH is greater than the pH_{zpc} that equal to 7.2 for natural clay, the negative charged clay surface is favorable for the adsorption MB dye. Özdemiş et al., also stated that clay surface exhibits positive zeta potential values at low pH (below pH 7.2), and with the increasing of pH, the surface of clay becomes more negatively charged, thereby increasing electrostatic attractions between positively charged dye anions (MB^+) and negatively charged clay causing increase in adsorption capacity.

3.3. Isotherm models

The experimental results indicated that the adsorption equilibrium data for the adsorption MB onto clay were fitted Langmuir, Freundlich, Temkin, and Redlich–Peterson isotherms.

In order to quantitatively compare the applicability of different models, the average relative error (ARE) was calculated using Eq. (2):

$$\text{ARE} = \frac{1}{N} \left[\sum_{i=1}^N \left| \frac{q_{e,\text{cal}} - q_{e,\text{exp}}}{q_{e,\text{exp}}} \right| \right] \quad (2)$$

where N is the number of data points, $q_{e,\text{exp}}$ and $q_{e,\text{cal}}$ (mg g^{-1}) are the experimental and the calculated values of the equilibrium adsorbate solid concentration in the solid phase, respectively. The values of ARE is used as measures of fitting the data to the isotherm equation, small values of ARE would indicate a perfect fit.

3.3.1. Langmuir isotherm

The Langmuir isotherm [27] is valid for monolayer adsorption on a homogenous adsorbent surface containing a finite number of identical site with no interaction between adsorbate molecules.

The Langmuir expression is represented by the following equation:

$$q_e = \frac{1 + K_L C_e}{1 + a_L C_e} \quad (3)$$

This may be converted into a linear form which is convenient for plotting and determining the constants K_L ($\text{dm}^3 \text{g}^{-1}$) and a_L ($\text{dm}^3 \text{mg}^{-1}$):

$$\frac{C_e}{q_e} = \frac{a_L}{K_L} C_e + \frac{1}{K_L} \quad (4)$$

The essential characteristics of the Langmuir isotherm can be expressed in terms of a dimensionless equilibrium parameter (R_L), which is defined by Hall et al. [28]:

$$R_L = \frac{1}{1 + K_L \cdot C_0} \quad (5)$$

where R_L is a dimensionless constant separation factor, C_0 is the initial concentration of dye (mg dm^{-3}) and K_L is the Langmuir adsorption constant ($\text{dm}^3 \text{g}^{-1}$).

The value of R_L indicates the shape of the isotherms to be either unfavorable ($R_L > 1$), linear ($R_L = 1$), favorable ($0 < R_L < 1$) or irreversible ($R_L = 0$). Linear plots of (C_e/q_e) versus (C_e) with high linear regression coefficient values ($R^2 > 0.999$) for adsorption MB onto clay at different temperatures, particle size and solution pH are obtained.

The values of K_L and a_L have been calculated for the different variables using Eq. (4) and listed with the corresponding values of linear regression coefficient (R^2) and the average relative of the errors function (ARE) in Table 2. The values of the constant (K_L/a_L) correspond to the maximum adsorption capacity (q_m) of the clay for MB were also calculated and listed in Table 2.

Table 2
Langmuir and freundlich parameters for the adsorption of MB onto natural clay at different variables

Parameter	Langmuir					Freundlich			
	K_L	a_L	q_m (mg g^{-1})	R^2	ARE	K_F	n	R^2	ARE
T ($^{\circ}\text{C}$)									
15	105.3	0.242	435.1	0.9998	0.1131	249.7	9.67	0.8994	0.0224
25	238.1	0.548	434.5	0.9995	0.2054	265.2	9.55	0.9555	0.0402
35	322.6	0.710	454.4	0.9997	0.1894	235.9	6.90	0.937	0.0803
45	384.6	0.808	476.0	0.9998	0.1735	296.4	10.00	0.9404	0.0460
dp μm									
80–125	196.1	0.431	455.0	0.9999	0.1002	261.5	9.07	0.9041	0.0613
250–355	238.1	0.548	434.5	0.9995	0.2054	265.2	9.55	0.9555	0.0402
500–710	101.0	0.242	417.4	0.9998	0.0540	221.4	8.14	0.8994	0.0452
pH									
2	384.6	0.962	399.8	0.9998	0.1138	293.0	15.95	0.868	0.0420
6	238.1	0.548	434.5	0.9995	0.2054	265.2	9.55	0.9555	0.0402
8	434.8	0.957	454.3	0.9999	0.1686	312.1	12.03	0.9351	0.0431
12	1000.0	2.000	500.0	1.0000	0.1394	289.1	8.67	0.8722	0.0975

It is clear from Table 2 that all variables play a strong role in the adsorption of MB. Increasing temperature from 15°C to 45°C led to an increase in the maximum adsorption capacity from 434.8 to 476.2 mg g⁻¹, suggests endothermic nature of the process. Increasing particle size ranges from 80–128 to 500–710 μm led to a decrease in the q_m from 455.0 to 417.4 mg g⁻¹. However, increasing solution pH from 2 to 12 led to increase q_m from 399.8 to 500.0 mg g⁻¹.

Values of R_L for natural MB/clay system have been calculated for the all variables and found that all values of R_L suggest favorable adsorption process ($0 < R_L < 1$). One example allowing an estimation of the R_L value is depicted in Fig. 7, which shows plots of R_L against initial MB concentrations at different temperatures. As shown in the Figure all values of R_L lies between 0 and 1, indicated that the favorability of the adsorption process. The Figure also shows that R_L value decreased with increasing initial MB concentrations suggested that adsorption process was more favorable at higher concentration.

Data in Table 3 indicated that Yemen natural clay has very high adsorption capacity compared to other adsorbents.

Table 3
Adsorption capacity (q_m) of methylene blue on to various adsorbents

Adsorbent	q_m (mg g ⁻¹)	Sources
Commercial activated carbon	980.3	Kannan and Sundaram [29]
Activated clay (Moroccan)	558.0	El Mouzdahir et al. [30]
Yemen natural clay	500.0	The present work
Straw activated carbon	472.1	Kannan and Sundaram [29]
Coconut husk-based activated carbon	434.8	Senthilkumaar et al. [21]
Activated carbon prepared from waste newspaper	390.0	Okada et al. [31]
Clay (Tunisia)	300.0	Bagane and Guiza [32]
Montmorillonite clay	289.1	Almedia et al. [33]
Activated carbon prepared from durian shell	289.3	Chandra et al. [34]
Activated sludge biomass	256.4	Gulnaz et al. [35]
Activated carbon prepared from oil palm shell	243.9	Senthilkumaar et al. [21]
Filtrisorb F300a	240.0	Stavropoulos [36]
Diatomite (Jordan)	198.0	Al-Ghouti et al. [37]
Perlite	162.3	[44] Dogan et al. [38]
Diatomite (Jordan)	156.6	Shawabkeh and Tutunji [39]
Bentonite	150.0	Hong et al. [40]
Bamboo dust-based activated carbon	143.2	Kannan and Sundaram [29]
Dehydrated peanut hull	123.5	Özer et al. [41]
Palygroskite	50.8	Al-Futaisi et al. [42]
Clay (Turkey)	6.3	Gurses et al. [43]

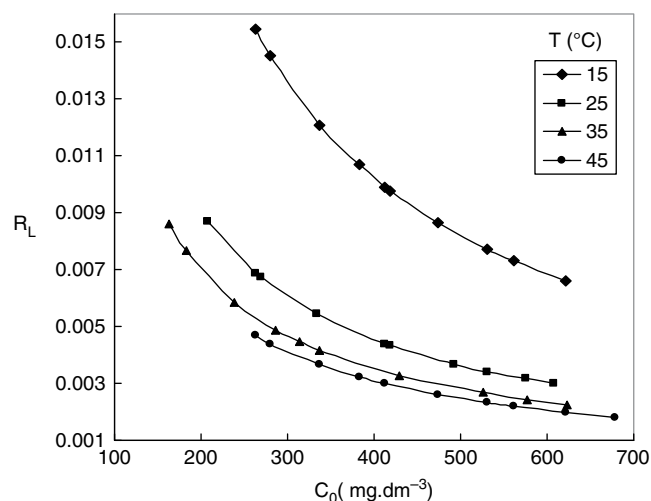


Fig. 7. Plot R_L against initial MB concentration at different temperatures.

3.3.2. Freundlich isotherm

The experimental equilibrium data for the adsorption of MB onto clay at different temperatures, particle

size and pH have been analyzed using the Freundlich isotherm as given by Eq. (6) [44]:

$$q_e = K_F C_e^{1/n} \quad (6)$$

where K_F is Freundlich constant ($\text{dm}^3 \text{g}^{-1}$) ^{n} and n is the heterogeneity factor. The K_F value is related to the adsorption capacity; while $1/n$ value is related to the adsorption intensity. The magnitude of exponent (n) gives an indication of the favorability and capacity of the adsorbent/adsorbate system. Values of (n) greater than 1 represent favorable adsorption according to Treybal [45].

Eq. (6) may be linearized via a logarithmic plot which enables the exponent (n) and the constant (K_F) to be determined:

$$\log q_e = \log K_F + (1/n) \log C_e \quad (7)$$

The Freundlich parameters (K_F and n) have been calculated using the least-squares method and are listed with the corresponding values of R^2 and ARE in Table 4.

According to the results shown in Table 4, the values of n are greater than unity indicating that the adsorption of MB onto clay is favorable. This is in great agreement with the findings regarding to R_L values.

3.3.3. Temkin isotherm

The Temkin isotherm has been used in the following form [46]:

$$q_e = \frac{RT}{b_T} (\ln A_T C_e) \quad (8)$$

Eq. (9) can be expressed in its linear form as:

$$q_e = B_T \ln A_T + B_T \ln (C_e) \quad (9)$$

where

$$B_T = \frac{RT}{b_T} \quad (10)$$

where T is the absolute temperature (K), R is the universal gas constant ($\text{J g mol}^{-1} \text{K}^{-1}$), A_T is the equilibrium binding constant corresponding to the maximum binding energy ($\text{dm}^3 \text{mg}^{-1}$), b_T is Temkin isotherm constant (J g mol^{-1}) and the constant B_T is related to the heat of adsorption (dimensionless). According to Eq. (9), a plot of (q_e) against $\ln(C_e)$ enables the determination of the isotherm constants (A_T and B_T). The values of A_T and B_T are calculated for different variables studied and listed with the corresponding values of R^2 and ARE in Table 4.

3.3.4. Redlich–Peterson isotherm

The Redlich–Peterson isotherm contains three parameters and involves the features of both the Langmuir and the Freundlich isotherms [47]. It can be described as follows:

$$q_e = \frac{(K_{RP} C_e)}{(1 + a_{RP} C_e^\beta)} \quad (11)$$

where K_{RP} is the modified Langmuir constant ($\text{dm}^3 \text{g}^{-1}$), a_{RP} ($\text{dm}^3 \text{mg}^{-1}$) and β are constant. $\beta \leq 1$.

Table 4

Temkin and redlich-peterson parameters for the adsorption of MB onto natural clay at different variables

Parameter	Temkin				Redlich-peterson				
	B_T	A_T	R^2	ARE	K_{RP}	a_{RP}	β	R^2	ARE
T(°C)									
15	34.93	980.3	0.9350	0.0183	1712.8	6.365	0.9130	0.9986	0.0177
25	33.87	2891.0	0.9817	0.0302	1800.0	5.200	0.9581	0.9995	0.0275
35	43.62	289.7	0.9854	0.0380	1905.3	6.368	0.9154	0.9999	0.0172
45	32.44	17222.6	0.9588	0.0376	1935.4	4.588	0.9837	0.9990	0.0371
dp μm									
80–125	37.41	1110.1	0.9430	0.0458	2010.5	6.920	0.9120	0.9993	0.0399
250–355	33.87	2891.0	0.9817	0.0302	1800.0	5.200	0.9581	0.9995	0.0275
500–710	39.87	186.8	0.9350	0.0406	940.7	3.904	0.8942	0.9986	0.0411
pH									
2	23.67	134787.3	0.9827	0.1379	1613.8	4.475	0.9828	0.9996	0.0246
6	33.87	2891.0	0.9817	0.0302	1800.0	5.200	0.9581	0.9995	0.0275
8	28.99	59610.2	0.9661	0.0326	2100.5	4.917	0.9914	0.9993	0.0291
12	40.13	2316.9	0.9287	0.0792	2100.5	4.917	0.9914	0.9995	0.0301

Eq. (12) is linear from which constants K_{RP} , a_{RP} and β can be determined:

$$\log \left(\frac{K_{RP} C_e}{q_e} - 1 \right) = \log a_{RP} + \beta \log C_e \quad (12)$$

Plotting $(\log [(K_{RP} C_e / q_e) - 1])$ against $(\log C_e)$ yields a straight line of slope = β and intercept = $\log a_{RP}$.

The isotherm parameters in Eq. (11) were calculated using Eq. (13) are listed with the corresponding values of R^2 and ARE in Table 4.

The results listed in Tables 2 and 4 indicated that Redlich–Peterson isotherm model fit the experimental data for the adsorption of MB onto natural clay at different temperature, particle size and pH better than Langmuir, Freundlich, and Temkin isotherms based on the very high values of R^2 ($R^2 > 0.999$) and lower values of ARE compared to other models.

3.4. Thermodynamic study

Feasibility and nature of any reaction can be explained better by studying the thermodynamics of the process. The thermodynamic parameters studied are changes in Gibbs free energy (ΔG°), standard enthalpy (ΔH°), and standard entropy (ΔS°).

The Gibbs free energy change of adsorption is defined as:

$$\Delta G^\circ = -2.303 RT \log K_L \quad (13)$$

where K_L is Langmuir equilibrium constant ($\text{dm}^3 \text{g}^{-1}$), (R) is the universal gas constant ($8.314 \text{ J g mol}^{-1} \text{ K}^{-1}$) and (T) is the absolute temperature (K).

The values of (ΔH°) and (ΔS°) were calculated using Van't Hoff equation:

$$\log K_L = \frac{\Delta S^\circ}{2.303R} - \frac{\Delta H^\circ}{2.303RT} \quad (14)$$

A plot of $(\log K_L)$ versus $(1/T)$ produce a straight line with slope equals to $-\Delta H^\circ / 2.303RT$ and intercept equals to $\Delta S^\circ / 2.303R$ [48]. Fig. 8 shows linear relation between $(\log K_L)$ and $(1/T)$ with high correlation coefficient ($R^2 > 0.9$). The values of (ΔH°) and (ΔS°) are calculated from the slope and the intercepts of straight line in Fig. 8 and listed in Table 5. The values of standard Gibbs free energy (ΔG°) are calculated using Eq. (13) and also listed in Table 5.

(ΔH°) and (ΔS°) were found to be $32.25 \text{ (kJ g mol}^{-1}\text{)}$ and $152.0 \text{ (J g mol}^{-1} \text{ K}^{-1}\text{)}$, respectively. The positive value of (ΔH°) indicates that the adsorption is an endothermic

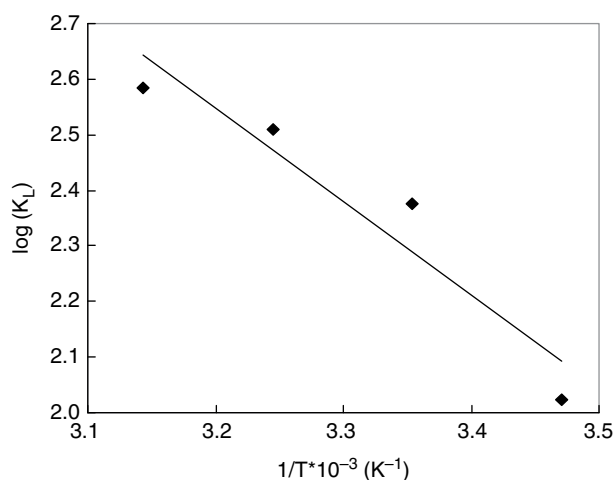


Fig. 8. Plot of $\log K_L$ against $1/T$ for the adsorption of MB onto clay. Particle diameter = $250\text{--}355 \mu\text{m}$, mass of clay = 0.05 g , $\text{pH} = 6 \pm 0.1$ and solution volume = 0.05 dm^3 .

Table 5

Thermodynamic parameters for the adsorption of MB onto natural clay

T (K)	ΔG° (kJ g mol ⁻¹)	ΔH° (kJ g mol ⁻¹)	ΔS° (J g mol ⁻¹ K ⁻¹)	R^2
288.15	-11.2	32.3	152.0	0.906
298.15	-13.6	–	–	–
308.15	-14.8	–	–	–
318.15	-15.7	–	–	–

process, and the positive value of (ΔS°) reflects the increased randomness at the solid/solution interface [49].

The negative values of (ΔG°) are indicative of spontaneous nature of the process of removal of dye by clay. The results in Table 5 show that the negative value of (ΔG°) increase with increase temperature, indicating that the spontaneous natures of adsorption of MB is in direct proportional to the temperature that is to say higher temperature favored the adsorption.

4. Conclusions

This study investigated the modeling of equilibrium and the thermodynamic of adsorption of methylene blue onto Yemen natural clay. The maximum adsorption capacity was found to vary with the temperature, clay particle size and pH. Maximum adsorption capacity increased from 435.1 to 476.0 mg g^{-1} with increasing temperature from 15°C to 45°C and increased from 417.4 to 455.0 mg g^{-1} with increasing pH from 2 to 12. However, the adsorption capacity decreased from 455.0 to 417.4 mg g^{-1} with increasing clay particle size from $80\text{--}125$ to $500\text{--}710 \mu\text{m}$. The Redlich–Peterson isotherm

was found to best fit the experimental data over the whole concentration range. The values of thermodynamic parameters ΔG° , ΔH° , and ΔS° indicated that the adsorption process is spontaneous, chemical in nature and favorable at high temperatures. The values of separation factor (R_L) revealed the favorable nature of the adsorption process of the MB/clay system ($0 < R_L < 1$). The study shows that Yemen natural clay can be used as low-cost adsorbent for the removal of methylene blue dye from aqueous solutions.

References

- [1] T. Robinson, G. McMullan, R. Marchant and P. Nigam, Remediation of dyes in textile effluent: a critical review on current treatment technologies with a proposed alternative, *Bioresour. Technol.*, 77 (2001) 247–255.
- [2] I.M. Banat, P. Nigam, D. Singh and R. Marchant, Microbial decolorization of textile-dye-containing effluents: a review, *Bioresour. Technol.*, 58 (1996) 217–227.
- [3] J. Yener, T. Kopac, G. Dogu and T. Dogu, Dynamic analysis of sorption of methylene blue dye on granular and powdered activated carbon, *Chem. Eng. J.*, 144 (2008) 400–410.
- [4] A.H. Konsowa, Bromate removal from water using granulated activated carbon in a batch recycle, *Desalin. Water Treat.*, 12 (2009) 375–381.
- [5] A.K. Jain, V.K. Gupta and A. Bhatnagar, Utilization of industrial waste products as adsorbents for removal of dyes, *J. Hazard. Mater.*, B101 (2003) 31–42.
- [6] I.G. Rashed, J. Akunna, M.M. El-Halawany and A.F. Abdou Atiaa, Improvement in the efficiency of hydrolysis of anaerobic digestion using enzymes *Desalin. Water Treat.*, 21 (2010) 1–6.
- [7] E.S.Z. Ashtoukhy, T.M. Zewail and N.K. Amin, Removal of dyes from aqueous solution by electrocoagulation using a horizontal expanded Ai-anode, *Desalin. Water Treat.*, 20 (2010) 72–79.
- [8] M.S. El-Geundi, Colour removal from textile effluents by adsorption techniques, *Water Res.*, 25 (1991) 271–273.
- [9] M.M. Nassar and Y.H. Magdy, Removal of different basic dyes from aqueous solutions by adsorption on palm-fruit bunch particles, *Chem. Eng. J.*, 66 (1997) 223–226.
- [10] B. Chen, C.W. Hui and G. McKay, Pore-surface diffusion modeling for dyes from effluent on pith, *Langmuir*, 17 (2001) 740–748.
- [11] B.H. Hameed and M.I. El-Khaiary, Malachite green adsorption by rattan sawdust: isotherm, kinetic and mechanism modeling, *J. Hazard. Mater.*, 159 (2008) 574–579.
- [12] B.H. Hameed, Evaluation of papaya seeds as a novel non-conventional low-cost adsorbent for removal of methylene blue, *J. Hazard. Mater.*, 162 (2009) 939–944.
- [13] M. Doğan, H. Abak and M. Alkan, Adsorption of methylene blue onto hazelnut shell: kinetics, mechanism and activation parameters, *J. Hazard. Mater.*, 164 (2009) 172–181.
- [14] K.G. Bhattacharyya and S.S. Gupta, Adsorption of a few heavy metals on natural and modified kaolinite and montmorillonite: a review, *Adv. Colloid Interface Sci.*, 140 (2008) 114–131.
- [15] P.H. Rao and M. He, Adsorption of anionic and nonionic surfactant mixtures from synthetic detergents on soils, *Chemosphere*, 63 (2006) 1214–1221.
- [16] M. Doğan, M. Hamdi, K. Karaoğlu and M. Alkan, Adsorption kinetics of maxilon yellow 4GL and maxilon red GRL dyes on kaolinite, *J. Hazard. Mater.*, 165 (2009) 1142–1151.
- [17] E.P. Barrett, L.G. Joyner and P.P. Halenda, The determination of pore volume and area distributions in porous substances, I. Computations from nitrogen isotherms, *J. Am. Chem. Soc.*, 73 (1951) 373–380.
- [18] S.J. Gregg and K.S.W. Sing, *Adsorption Surface Area and Porosity*, 2nd ed., Academic Press, London, 1982.
- [19] C.H. Gilles, T.H. Macewan, S.N. Nakhwa and D. Smith, A system of classification of solution adsorption isotherms, and its use in diagnosis of adsorption mechanisms, *J. Chem. Soc.*, 4 (1960) 3973–3993.
- [20] S. Wang and Z.H. Zhu, Effects of acidic treatment of activated carbons on dye adsorption, *Dyes Pigments*, 75 (2007) 306–314.
- [21] P.R. Senthilkumar, P.R. Varadarajan, K. Porkodi and C.V. Subburaam, Adsorption of methylene blue onto jute fiber carbon: kinetics and equilibrium studies, *J. Colloid Interface Sci.*, 284 (2005) 78–82.
- [22] R. Han, J. Zhang, P. Han, Y. Wang, Z. Zhao and M. Tang, Study of equilibrium, kinetic and thermodynamic parameters about Methylene Blue adsorption onto natural zeolite, *Chem. Eng. J.*, 145 (2009) 496–504.
- [23] Y.C. Wong, Y.S. Szeto, W.H. Cheung and G. McKay, Effect of temperature, particle size and percentage deacetylation on the adsorption of acid dyes on chitosan, *Adsorption*, 14 (2008) 11–20.
- [24] V. Ponnusami, S. Vikram and S.V. Srivastava, Guava (*Psidium guajava*) leaf powder: novel adsorbent for removal of methylene blue from aqueous solutions, *J. Hazard. Mater.*, 152 (2008) 276–286.
- [25] Y. Al-Degs, M.A.M. Khraisheh, J.S. Allen and M.N. Ahmad, Effect of carbon surface chemistry on the removal of reactive dyes from textile effluent, *Water Res.*, 34 (2000) 927–935.
- [26] Y. Özdemir, M. Doğan and M. Alkan, Adsorption of cationic dyes from aqueous solutions by sepiolite, *Microporus Mesoporus Mater.*, 96 (2006) 419–427.
- [27] I. Langmuir, The constitution and fundamental properties of solids and liquids, *J. Am. Chem. Soc.*, 38 (1916) 2221–2295.
- [28] K.R. Hall, L.C. Eagleton, A. Acrivos and T. Vermeulen, Pore and solid-diffusion kinetics in fixed-bed adsorption under constant-pattern conditions, *Ind. Eng. Chem. Fundam.*, 5 (1966) 212–223.
- [29] H.M.F. Freundlich, Over the adsorption in solution, *J. Phys. Chem.*, 57 (1906) 385–470.
- [30] R.E. Treybal, *Mass transfer operation*, 3rd ed., McGraw-Hill, New York, 1985.
- [31] M.I. Temkin, Adsorption equilibrium and the kinetics of processes on nonhomogeneous surfaces and in the interaction between adsorbed molecules, *Zh. Fiz. Khim.*, 15 (1941) 296–332.
- [32] O. Redlich and D.L. Peterson, A useful adsorption isotherm, *J. Phys. Chem.*, 63 (1959) 1024–1029.
- [33] C.W. Cheung, J.F. Porter and G. McKay, Sorption kinetic analysis for the removal of cadmium ions from effluents using bone char, *Water Res.*, 35 (2001) 605–612.
- [34] J.M. Smith and H.C. Van Ness, *Introduction to Chemical Engineering Thermodynamics*, 4th ed., McGraw-Hill, Singapore, 1987.
- [35] N. Kannan and M.M. Sundaram, Kinetics and mechanism of removal of methylene blue by adsorption on various carbons—a comparative study, *Dyes Pigments*, 51 (2001) 25–40.
- [36] Y. El Mouzdahir, A. Elmchaouri, R. Mahboub, A. Gil and S.A. Korili, Equilibrium modeling for the adsorption of methylene blue from aqueous solutions on activated clay minerals, *Desalination*, 250 (2010) 335–338.
- [37] K. Okada, N. Yamamoto and Y. Kameshima, Adsorption properties of activated carbon from waste newspaper prepared by chemical and physical activation, *J. Colloid Interface Sci.*, 262 (2002) 194–199.
- [38] M. Bagane and S. Guiza, Removal of a dye from textile effluents by adsorption, *Ann. Chim. Sci. Mat.*, 25 (2000) 615–626.
- [39] C.A.P. Almeida, N.A. Debacher, A.J. Downs, L. Cottet and C.A.D. Mello, Removal of methylene blue from colored effluents by adsorption on montmorillonite clay, *J. Colloid Interface Sci.*, 332 (2009) 46–53.
- [40] T.C. Chandra, M.M. Mirna, Y. Sudaryanto and S. Ismadji, Adsorption of basic dye onto activated carbon prepared from durian shell: studies of adsorption equilibrium and kinetics, *Chem. Eng. J.*, 127 (2007) 121–129.

- [41] O. Gulnaz, A. Kaya, F. Matyar and B. Arikian, Sorption of basic dyes from aqueous solution by activated sludge, *J. Hazard. Mater.*, B108 (2004) 183–188.
- [42] G.G. Stavropoulos and A.A. Zabaniotou, Production and characterization of activated carbons from olive-seed waste residue, *Microporus Mesoporus Mater.*, 82 (2005) 79–85.
- [43] M.A. Al-Ghouti, M.A.M. Khraisheh, S.J. Allen and M.N. Ahmad, The removal of dyes from textile wastewater: a study of the physical characteristics and adsorption mechanisms of diatomaceous earth, *J. Environ. Manage.*, 69 (2003) 229–238.
- [44] M. Dogan, M. Alkan and Y. Onager, Adsorption of methylene blue from aqueous solution onto perlite, *Water Air Soil Pollut.*, 120 (2000) 229–248.
- [45] R.A. Shawabkeh and M.F. Tutunji, Experimental study and modeling of basic dye sorption by diatomaceous clay, *Appl. Clay Sci.*, 24 (2003) 111–120.
- [46] S. Hong, C. Wen, J. He, F. Gan and Y.S. Ho, Adsorption thermodynamics of methylene blue onto bentonite, *J. Hazard. Mater.*, 167 (2009) 630–633.
- [47] D. Ozer, G. Dursun and A. Ozer, Methylene Blue adsorption from aqueous solution by dehydrated peanut hull, *J. Hazard. Mater.*, 144 (2007) 171–179.
- [48] A. Al-Futaisi, A. Jamrah and R. Al-Hanai, Aspects of cationic dye molecule adsorption to palygorskite, *Desalination*, 214 (2007) 327–342.
- [49] A. Gurses, S. Karaca, C. Dogar, R. Bayrak, M. Acikydiz and M. Yalcin, Determination of adsorptive properties of clay/water system: methylene blue sorption, *J. Colloid interface Sci.*, 269 (2004) 310–314.